Journal Pre-proofs



Perspective

Towards multicolor tin-based perovskite light-emitting diodes

Yuxin Shi, Qingsen Zeng, Tae-Woo Lee

PII: S2095-9273(26)01339-3
DOI: https://doi.org/10.1016/j.scib.2026.10.068
Reference: SCIB 4502

To appear in: *Science Bulletin*

Please cite this article as: Y. Shi, Q. Zeng, T-W. Lee, Towards multicolor tin-based perovskite light-emitting diodes, *Science Bulletin* (2026), doi: https://doi.org/10.1016/j.scib.2026.10.068

This is a PDF of an article that has undergone enhancements after acceptance, such as the addition of a cover page and metadata, and formatting for readability. This version will undergo additional copyediting, typesetting and review before it is published in its final form. As such, this version is no longer the Accepted Manuscript, but it is not yet the definitive Version of Record; we are providing this early version to give early visibility of the article. Please note that Elsevier's sharing policy for the Published Journal Article applies to this version, see: https://www.elsevier.com/about/policies-and-standards/sharing#4-published-journal-article. Please also note that, during the production process, errors may be discovered which could affect the content, and all legal disclaimers that apply to the journal pertain.

© 2026 The Authors. Published by Elsevier B.V. and Science China Press

Towards multicolor tin-based perovskite light-emitting diodes

*Yuxin Shi[1], Qingsen Zeng[1,2], and Tae-Woo Lee[1,2,3,4,]**

[1]Department of Materials Science and Engineering, Seoul National University, Seoul 08826, Republic of Korea.

[2]Research Institute of Advanced Materials (RIAM), Seoul National University, Seoul 08826, Republic of Korea.

[3]Institute of Engineering Research, Interdisciplinary Program in Bioengineering, Soft Foundry, SN Display Co., Ltd., Seoul National University, Seoul 08826, Republic of Korea.

[4]SN Display Co., Ltd., Seoul 08826, Republic of Korea.

*Corresponding author. E-mail: twlees@snu.ac.kr

Metal halide perovskite light-emitting diodes (PeLEDs) have advanced rapidly over the past decade, with lead (Pb)-based systems now achieving external quantum efficiencies (EQEs) exceeding 20% and emission spanning the visible to near-infrared (NIR) spectrum [1]. The remarkable success of Pb-based PeLEDs stems from their excellent optoelectronic properties and the versatility of compositional and dimensional engineering, which allow precise control over phase architectures and predictable emission-color tuning across a broad spectral range. Despite this progress, concerns regarding lead toxicity, environmental regulations, and long-term sustainability continue to motivate the development of high-performance lead-free alternatives.

Tin (Sn)-based perovskites have therefore emerged as particularly compelling alternatives owing to their similar electronic configurations and broadly comparable band structures [2]. Because of the delocalized, stereochemically active $5s^2$ lone-pair electrons and strong Sn 5s–halide p orbital hybridization, Sn-based perovskites possess stronger Sn–X (X = halide) covalency and intrinsically softer lattices than their Pb-based counterparts. Consequently, their electronic structures are highly sensitive to local coordination environments, lattice strain, octahedral distortion, and dynamic structural fluctuations. In particular, high-energy emissive states—commonly associated with small-*n* phases (*n* is the number of inorganic layers), quantum-confined domains, or strained lattice configurations—are thermodynamically metastable and tend to relax toward energetically favored bulk-like structures with larger-*n* phases. This relaxation progressively biases emission toward the red-to-NIR region [3]. Therefore, the central challenge in achieving multicolor emission in Sn-based PeLEDs does not primarily arise from limited bandgap tunability, but from the difficulty of stabilizing metastable emissive states.

This challenge is further amplified by the intrinsic defect states of Sn-based perovskites. The low formation energy of Sn vacancies, together with the low redox potential of Sn^{2+}, makes Sn^{2+} highly susceptible to oxidation during film processing and device operation. Oxidation-induced Sn^{4+} defects introduce deep trap states that strongly enhance nonradiative recombination and accelerate exciton quenching. Empirically, the metastable small-*n* phases required for shorter-wavelength emission often suffer from increased trap-assisted recombination, lower photoluminescence

Journal Pre-proofs

quantum yields (PLQYs), and pronounced spectral broadening compared with their deep-red or NIR counterparts [4]. In addition, the strong Lewis acidity and high chemical reactivity of Sn^{2+} promote rapid nucleation and poorly controlled crystallization, frequently resulting in inferior crystallinity and elevated defect densities relative to Pb-based analogs.

To mitigate these issues, extensive efforts have focused on suppressing Sn^{2+} oxidation, passivating defects, and regulating crystallization kinetics through additive engineering (e.g., valeric acid, cyanuric acid, and vitamin B1), tin compensation (e.g., Sn powder and SnX_2, where X = F, Cl, Br, I, or SCN), and solvent coordination (e.g., dimethylformamide, dimethyl sulfoxide (DMSO), and antisolvents). These approaches have substantially improved red and NIR Sn-based PeLEDs, with reported EQEs exceeding 20% and luminance surpassing 8000 cd m^{-2} (Fig. 1a). However, additives such as SnF_2 mainly suppress Sn^{2+} oxidation and passivate vacancy defects rather than directly regulating nucleation. Studies show that SnF_2 also promotes bulk-like grain growth [5] and, at high concentrations, phase separation, biasing the system toward larger, thermodynamically favored domains rather than the small-*n*, high-energy phases needed for blue/green emission. Efficient multicolor electroluminescence therefore remains difficult because existing strategies mainly improve defect tolerance and red/NIR emission but do not sufficiently stabilize metastable high-energy emissive states (Fig. 1b).

Fig. 1. Development and emission characteristics of Sn-based PeLEDs. (a) Evolution of EQE, luminance, and radiance over time. (b) EQE as a function of electroluminescence wavelength for reported Sn-based PeLEDs. Blue emission mainly originates from Br-rich 2D phases, red emission from Br/I-based 2D and 3D phases, and NIR emission from I-rich 3D phases. (c) Energy-level diagrams of representative Sn-based PeLEDs.

In principle, compositional engineering modifies the orbital interactions between Sn and halide ions, thereby tuning the bandgap over a broad spectral range. Sn 5p orbitals play a major role in forming the conduction band, while the valence band originates from antibonding interactions involving Sn 5s and halide *n*p orbitals (Cl 3p, Br 4p, I 5p). Consequently, halide and cation substitution can theoretically regulate the bandgap from the NIR to the visible region, from approximately 1.2 to beyond 3 eV (Fig. 1c).

Experimentally, most reported Sn-based PeLEDs still exhibit red-to-NIR emission, primarily in iodide-rich systems such as $CsSnI_3$ and mixed formamidinium (FA)/methylammonium (MA)/Cs Sn iodides. Although partial Br substitution can progressively blue-shift the emission—for example, from ~950 to ~675 nm in the $CsSn(I/Br)_y$ system [3]—increasing halide heterogeneity frequently induces phase segregation, defect formation, and local compositional fluctuations under electrical bias. These effects destabilize high-energy emissive domains and broaden the emission spectrum. Halide chemistry thus defines the accessible spectral window rather than deterministically controlling the final emissive state.

Among Sn-based perovskites, $FASnI_3$ generally resists Sn^{2+} oxidation better than $MASnI_3$ and has therefore been widely studied as a representative composition. However, the large FA^+ cation gives

$FASnI_3$ a tolerance factor (t) of 1.04, which causes phase instability and poor crystallinity. Mixing FA^+ with other monovalent cations (e.g., MA^+ and Cs^+) is therefore a promising strategy [6]. For example, $FA_{1-x}MA_xSnBr_3$ adopts a cubic structure whose lattice parameter and cell volume obey Vegard's law, and FA^+/MA^+ substitution tunes the bandgap from 2.4 to 1.9 eV, possibly because FA^+ and MA^+ influence the defect density and, in turn, the valence-band characteristics (Fig. 2a).

Unlike Pb-based perovskites, where halide composition predictably sets the emission wavelength, Sn-based perovskites have stronger Sn–X covalency and softer lattices, making their electronic structures sensitive to local coordination and lattice strain, not composition alone. Dimensionality and lattice constraint must therefore be considered together with composition.

To date, most reported Sn-based PeLEDs have focused on 3D phases and predominantly exhibit NIR emission. The continuous lattice network of 3D perovskites enables efficient charge transport, as recently shown in a 3D Sn–Pb hybrid perovskite with carrier mobility exceeding 50 $cm^2\ V^{-1}\ s^{-1}$ [7]. Nevertheless, pure 3D Sn-based perovskites still suffer from limited carrier mobility and inadequate long-term stability, mainly because of Sn^{2+} oxidation and poorly controlled crystal growth during film formation. Incorporating bulky organic ammonium cations—such as 2-thiopheneethylammonium (TEA^+), phenethylammonium (PEA^+), 3-methoxyphenethylammonium ($MOPA^+$), and 7-(thiophen-2-yl)benzothiadiazol-4-yl)-[2,2′-bithiophen]-5-yl)ethylammonium (BTm^+)—can induce a dimensional transition from 3D to layered 2D structures (Fig. 2b) [8]. Reduced dimensionality introduces both quantum and dielectric confinement effects, substantially increasing exciton binding energies and promoting radiative recombination.

Indeed, isolated demonstrations of short-wavelength electroluminescence have been reported in low-dimensional Sn-based perovskites. For example, blue electroluminescence (~467 nm) was achieved in the 2D perovskite $(BrPMA)_2SnBr_4$, where $BrPMA^+$ is 4-bromophenylmethylammonium, with an EQE of 1.3% and a luminance of 800 cd m^{-2} [9]. These results suggest that dimensional engineering, together with halide regulation, represents a viable route toward overcoming the intrinsic long-wavelength emission tendency of Sn-based systems.

In quasi-2D systems, excitonic confinement can be coupled with energy funneling, in which photoexcited carriers migrate from small-n, wide-bandgap domains to larger-n emissive phases, providing access to higher-energy emission that is difficult to stabilize in bulk-like 3D Sn-based perovskites. However, quasi-2D Sn-based perovskites typically contain broad distributions of coexisting n-phases, leading to multiple emissive channels, heterogeneous recombination, spectral broadening, and poor operational stability. Because the final phase distribution is highly sensitive to crystallization pathways, dimensional engineering cannot be treated in isolation but is intrinsically coupled to nucleation, crystal growth, and phase evolution.

Lattice constraint, which arises from octahedral tilting, internal strain, and steric interactions with A-site or spacer cations (Fig. 2c), modifies the local structure with minimal change in overall composition, enabling continuous tuning of emissive states. Such regulation is particularly effective in Sn-based systems because their soft Sn–X framework is highly susceptible to structural fluctuations. Variations in Sn–X bond angles directly perturb the antibonding Sn 5s–X p states at the valence band while leaving the conduction band comparatively unaffected, allowing continuous

bandgap modulation and fine color tuning. Well-designed lattice constraints can also suppress dynamic disorder and spectral broadening, which is especially important for stabilizing shorter-wavelength emission.

Experimental evidence further supports this perspective. Nishimura et al. [10] engineered $Q_x(FA_{0.75}MA_{0.25})_{1-x}SnI_3$ films, where Q is a cation of varying ionic radius (Na^+, K^+, Cs^+, ethylammonium (EA^+), or butylammonium), and found that lattice strain decreases as t approaches unity. Among all the tested cations, the EA^+-containing film exhibited the lowest strain (~0.85%), with t closest to 1, and the highest measured carrier mobility of 43.03 $cm^2\ V^{-1}\ s^{-1}$, indicating that controlled lattice regulation suppresses structural disorder. Likewise, A-site cation substitution in $MA_{1-x}Cs_xSnBr_3$ and $MA_{1-x}Cs_xSnI_3$—which tunes both t and lattice distortion—enables continuous photoluminescence (PL) tuning from 560 to 685 nm (bandgap 1.8–2.15 eV), with PL intensity rising as lattice symmetry increases [11]. Consistently, energetic-disorder analyses attribute Urbach-tail broadening in Sn-based perovskites primarily to lattice strain and Sn-induced distortion rather than dynamic phonon effects, directly linking lattice quality to emission efficiency.

These factors are not independent variables but are all strongly mediated by crystallization kinetics during film formation, as confirmed in quasi-2D Sn-based perovskites incorporating 4-fluorophenethylammonium ($4FPEA^+$). Relative to conventional PEA^+, $4FPEA^+$ yields a near-180° out-of-plane Sn–I–Sn bond angle and suppresses octahedral distortion. Under optimized precursor stoichiometry and solvent conditions, this enables the isolation of phase-pure n = 2 and n = 3 structures with prolonged air stability and, for n = 2, lower amplified spontaneous emission thresholds [12]. The steric and electronic characteristics of spacer cations, together with crystallization conditions, thus jointly govern dimensional phase selection and lattice geometry.

Fig. 2. Strategies for stabilizing Sn-based perovskites and improving film and device performance. Schematic illustration of (a) compositional engineering (M = other metal cation), (b) dimensionality, and (c) lattice distortion/lattice constraint in Sn-based perovskites. (d) Model for nucleation and growth of perovskite crystals in precursor solution, relationship between nucleation radius and Gibbs free energy, and crystal growth on the particle surface. (e) Representative coordination-regulated principles for stabilizing Sn^{2+} in Sn-based perovskites. (f) t plotted against PLQY, FWHM, EQE, and radiance for representative Sn-based PeLEDs.

According to classical nucleation theory ($\Delta\mu \propto 2\gamma/r$, where γ is the surface energy and r is the particle radius), small crystallites possess higher chemical potential and are therefore thermodynamically metastable, driving Ostwald ripening toward larger grains [13]. Forming a stable nucleus requires overcoming a Gibbs free energy barrier (ΔG_c), which depends sensitively on supersaturation, interfacial energy, and local chemical environment. In real thin films, heterogeneous nucleation dominates, occurring at substrates, buried interfaces, or defect sites; by locally lowering this barrier, interfaces can stabilize strained lattices, reduced-dimensional motifs, or halide-rich environments that emit at shorter wavelengths but would be disfavored in bulk equilibrium. This classical picture, however, assumes a well-defined monomeric precursor. In practice, Sn-halide precursor solutions contain a distribution of soluble complexes and intermediate Sn–solvent or Sn–halide species,

whose stability and interconversion rate determine the supersaturation available for nucleation [14]. This offers a chemistry-based lever over the nucleation barrier beyond classical particle-size arguments.

Following nucleation, crystal growth is either reaction-controlled or diffusion-controlled, depending on whether surface incorporation or monomer diffusion is rate-limiting [15]. In Sn-based perovskites, diffusion-controlled growth amplifies local variations in halide composition, lattice strain, and dimensionality, producing heterogeneous emissive domains, spectral broadening, and poor reproducibility. Reaction-controlled growth, by contrast, yields more uniform lattice evolution, narrower emission linewidths, and more homogeneous electroluminescence. This sensitivity explains why solvent engineering, drying dynamics, and additive chemistry can cause pronounced color variations even in nominally identical compositions (Fig. 2d). The kinetic picture is particularly acute for Sn. Theoretical calculations show that the $SnI_2 \cdot 3DMSO$ precursor solvate has a cohesive energy of −1.920 eV, substantially less negative than the −2.592 eV of the $PbI_2 \cdot 4DMSO$ solvate [14], owing to the stereochemically active lone pair on Sn^{2+}, which prevents Sn^{2+} from forming complexes with multiple Lewis-base ligands, such as DMSO, that are as stable as those formed by Pb^{2+}. Since crystallization proceeds through decomplexation of these solvates, the weaker Sn–solvent coordination is expected to lower the decomplexation barrier, driving faster and less controllable crystallization in Sn-based systems.

In Sn-based perovskites, coordination-regulated crystallization is particularly important because it can kinetically stabilize strained, low-dimensional, or halide-heterogeneous domains that would otherwise relax toward lower-energy emissive states. Through Lewis acid–base interactions with Sn species, coordinating additives and ligands modulate precursor complexation and supersaturation evolution, enabling more controlled nucleation and intermediate-phase formation (Fig. 2e). SnX_2 additives, particularly SnF_2, are widely employed to suppress Sn^{2+} oxidation, defect formation, and secondary phases, but excessive amounts cause aggregation, phase segregation, and poorer film quality. To regulate the local coordination environment of Sn species more precisely, various additives and ligands have therefore been developed. Functional groups bearing lone pairs (e.g., C=O, C=N, C=S, O–H, and N–H) coordinate with Sn^{2+}, while π-conjugated frameworks promote electron delocalization and electronic stabilization. The steric configuration of these molecules can further tune their binding strength toward Sn species [16].

During spin-coating, strong coordination stabilizes intermediate Sn–additive or Sn–ligand complexes, slows precursor conversion, reduces the effective supersaturation, and suppresses uncontrolled heterogeneous nucleation. During annealing, residual additives and ligands further stabilize intermediate phases and retard crystal growth as the solvent is removed, guiding oriented growth and enlarging grains. For example, SCN^--containing salts suppress the crystallization rate and promote vertical crystal orientation. In antisolvent-assisted spin-coating, rapid solvent extraction promotes the replacement of coordinated solvent molecules by ligands around Sn-containing colloidal complexes, facilitating nucleation and growth.

We further tested whether static lattice distortion dominates the emission properties of Sn-based perovskites, in which case performance should improve systematically as *t* approaches the favorable

range. Plotting t for representative Sn-based emitters against reported EQE, radiance, PLQY, and full width at half maximum (FWHM) (Fig. 2f) shows higher PLQY and EQE for several compositions near $t \approx 0.9–1.0$, consistent with reduced static distortion. However, the substantial scatter and the absence of monotonic relationships between t and either FWHM or radiance indicate that t alone does not predict emission properties. Static lattice geometry must therefore be considered together with dynamic disorder and crystallization-dependent phase heterogeneity when stabilizing metastable emissive states.

Looking forward, color control in Sn-based PeLEDs should be viewed as a non-equilibrium state engineering challenge, with three priorities. First, metastable emissive states should be kinetically stabilized. Rather than simply tuning the bandgap to shorter wavelengths, nucleation and growth pathways should be designed to trap high-energy emissive domains, such as low-dimensional phases, strained lattices, or halide-heterogeneous regions, before they relax into thermodynamically preferred red/NIR states. This requires controlling the timing and location of nucleation, the supersaturation profile during spin-coating and annealing, and the rate of solvent removal. Second, composition, dimensionality, and lattice constraint should be controlled in a coupled manner. A single A-site or spacer cation can simultaneously modulate the tolerance factor, lattice strain, phase distribution, and coordination strength, which reduces the degrees of freedom in optimization and makes multicolor emission more predictable. Third, dynamic structural evolution during operation must be suppressed. Even a well-formed emissive state remains vulnerable to ion migration, phase segregation, Sn^{2+} oxidation, and lattice relaxation under electrical bias, calling for strategies such as cross-linking organic spacers, protecting Sn^{2+} with strongly coordinating ligands, and introducing interfacial layers that block ion migration. Realizing efficient and stable multicolor emission would extend Sn-based PeLEDs beyond red/NIR devices toward lead-free full-color displays and flexible light sources.

Conflict of interest

The authors declare that they have no conflict of interest.

Acknowledgments

This work was financially supported by the National Research Foundation of Korea (NRF) and the Ministry of Science, ICT & Future Planning (RS-2025-00560490).

References

[1] Cho H, Jeong S, Park M, et al. Overcoming the electroluminescence efficiency limitations of perovskite light-emitting diodes. Science 2015;350:1222-1225.
[2] Han D, Wang J, Agosta L, et al. Tautomeric mixture coordination enables efficient lead-

free perovskite LEDs. Nature 2023;622:493-498.
[3] Hong W, Lo P, Chiu H, et al. The influence of spontaneous oxidative conversion on the characteristics of lead-free halide perovskite $CsSn(I_xBr_{1-x})_3$ and on the performance of perovskite light-emitting diodes. Adv Mater Interfaces 2021;8:2002240.
[4] Treglia A, Ambrosio F, Martani S, et al. Effect of electronic doping and traps on carrier dynamics in tin halide perovskites. Mater Horiz 2022;9:1763-1773.
[5] Chen Q, Luo J, He R, et al. Unveiling roles of tin fluoride additives in high-efficiency low-bandgap mixed tin-lead perovskite solar cells. Adv Energy Mater 2021;11:2101045.
[6] Li P, Cao X, Li J, et al. Ligand engineering in tin-based perovskite solar cells. Nano-Micro Lett 2023;15:167.
[7] Wu Y, Yuan F, Yang S, et al. Tailoring tin-based perovskite crystallization via large cations and pseudo-halide anions for high mobility and high stable transistors. Sci Adv 2025;11:eadv4138.
[8] Min H, Wang N, Chen N, et al. Spin coating epitaxial heterodimensional tin perovskites for light-emitting diodes. Nat Nanotechnol 2024;19:632-637.
[9] Han Y, Guo Z, Liu S, et al. Manipulating electron-phonon coupling for efficient tin halide perovskite blue LEDs. Adv Mater 2025;37:2413895.
[10] Nishimura K, Hirotani D, Kamarudin M, et al. Relationship between lattice strain and efficiency for Sn-perovskite solar cells. ACS Appl Mater Interfaces 2019;11:31105-31110.
[11] Li M, Luo J, He J, et al. Bandgap engineering based on A-site ions tuning in tin halide perovskite. Small 2025;21:2409546.
[12] Triggs C, Wu C, He Y, et al. Cage balancing enhances optoelectronic and lasing performance in stable quasi-2D tin iodide perovskites. J Am Chem Soc 2025;147:34706-34720.
[13] Yin M, Yao H, Qiu H, et al. A revisit of crystallization in tin halide perovskite thin films: from nucleation, intermediate to crystal growth. Adv Funct Mater 2024;34:2404792.
[14] Jung M, Ji S, Kim G, et al. Perovskite precursor solution chemistry: from fundamentals to photovoltaic applications. Chem Soc Rev 2019;48:2011-2038.
[15] Schmidt-Mende L, Dyakonov V, Olthof S, et al. Roadmap on organic-inorganic hybrid perovskite semiconductors and devices. APL Mater 2021;9:109202.
[16] Gao W, Huang R, Dong H, et al. Heteroatomic molecules for coordination engineering towards advanced Pb-free Sn-based perovskite photovoltaics. Chem Soc Rev 2025;54:1384-1428.

Journal Pre-proofs

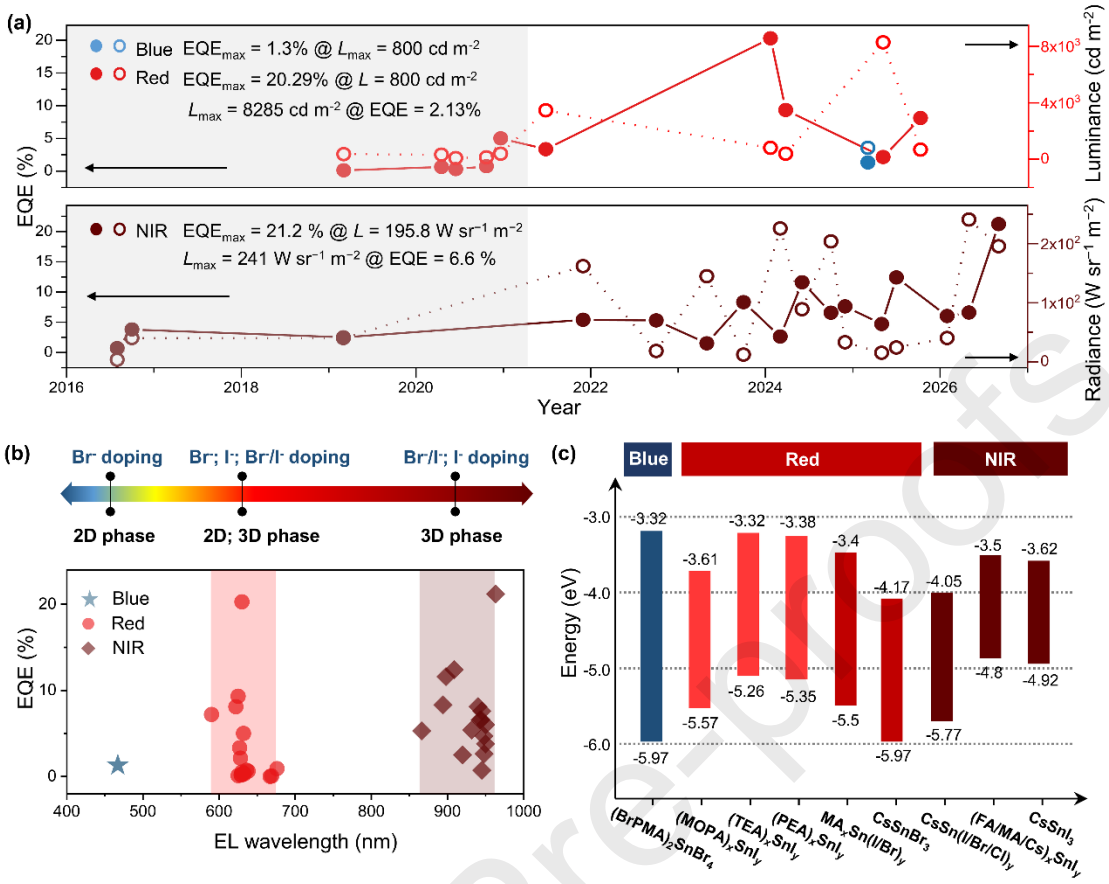

Journal Pre-proofs

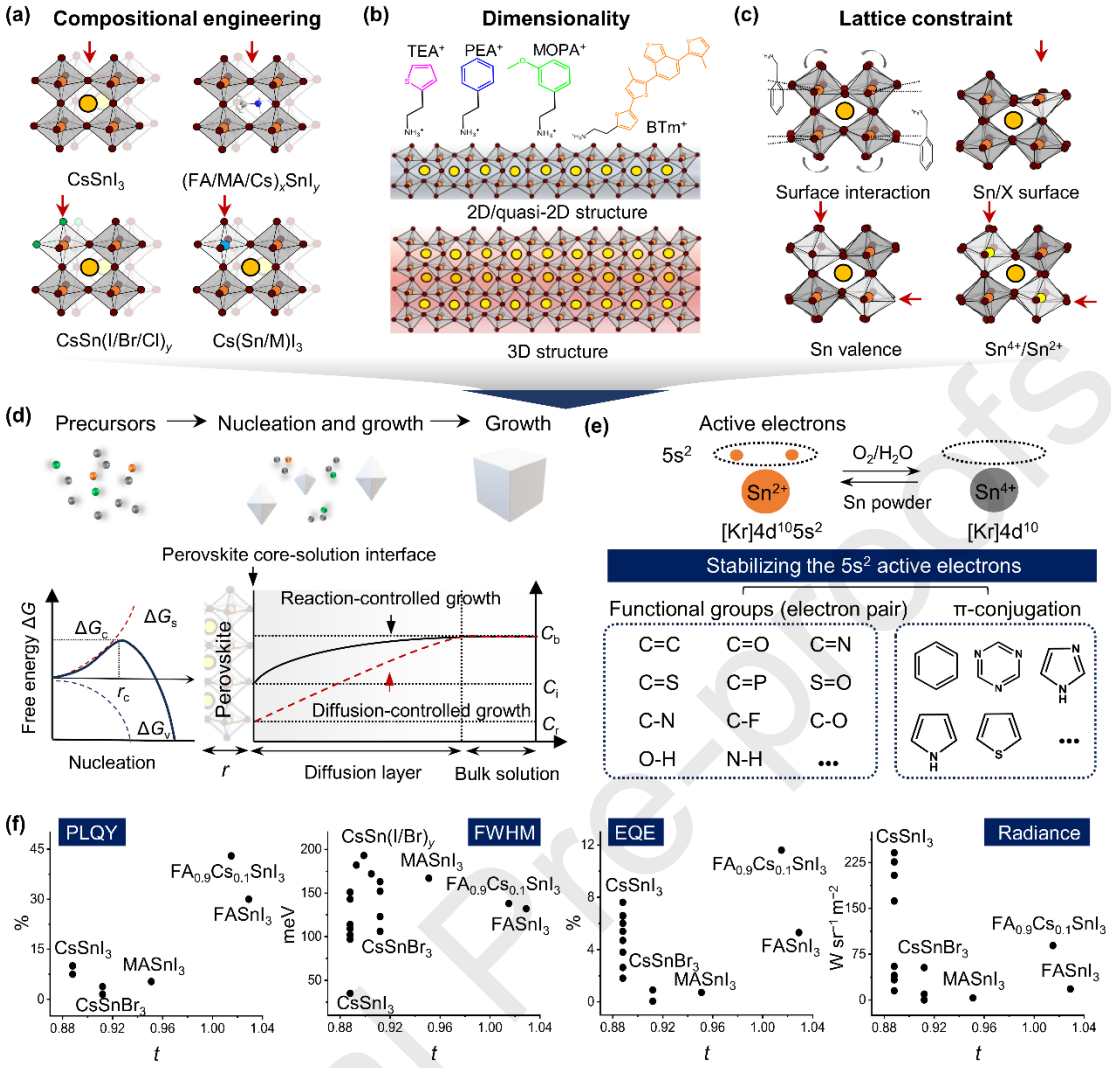

Journal Pre-proofs